Modeling of cosmic-ray anisotropy at TeV energies in an MHD model heliosphere

T. K. Sako
on behalf of the Tibet ASγ Collaboration
CRA 2023, May 16-19

Tibet ASγ Collaboration

M. Amenomori[1], S. Asano[2], Y. W. Bao[3], X. J. Bi[4], D. Chen[5], T. L. Chen[6], W. Y. Chen[4], Xu Chen[4,5], Y. Chen[3], Cirennima[6], S. W. Cui[7], Danzengluobu[6], L. K. Ding[4], J. H. Fang[4,8], K. Fang[4], C. F. Feng[9], Zhaoyang Feng[4], Z. Y. Feng[10], Qi Gao[6], A. Gomi[11], Q. B. Gou[4], Y. Q. Guo[4], Y. Y. Guo[4], Y. Hayashi[2], H. H. He[4], Z. T. He[7], K. Hibino[12], N. Hotta[13], Haibing Hu[6], H. B. Hu[4], K. Y. Hu[4,8], J. Huang[4], H. Y. Jia[10], L. Jiang[4], P. Jiang[5], H. B. Jin[5], K. Kasahara[14], Y. Katayose[11], C. Kato[2], S. Kato[15], I. Kawahara[11], T. Kawashima[15], K. Kawata[15], M. Kozai[16], D. Kurashige[11], Labaciren[6], G. M. Le[17], A. F. Li[4,9,18], H. J. Li[6], W. J. Li[4,10], Y. Li[5], Y. H. Lin[4,8], B. Liu[19], C. Liu[4], J. S. Liu[4], L. Y. Liu[5], M. Y. Liu[6], W. Liu[4], H. Lu[4], X. R. Meng[6], Y. Meng[4,8], K. Munakata[2], K. Nagaya[11], Y. Nakamura[15], Y. Nakazawa[20], H. Nanjo[1], C. C. Ning[6], M. Nishizawa[21], R. Noguchi[11], M. Ohnishi[15], S. Okukawa[11], S. Ozawa[22], X. Qian[5], X. L. Qian[23], X. B. Qu[24], T. Saito[25], Y. Sakakibara[11], M. Sakata[26], T. Sako[15], T. K. Sako[15], T. Sasaki[12], J. Shao[4,9], M. Shibata[11], A. Shiomi[20], H. Sugimoto[27], W. Takano[12], M. Takita[15], Y. H. Tan[4], N. Tateyama[12], S. Torii[28], H. Tsuchiya[29], S. Udo[12], H. Wang[4], S. F. Wang[6], Y. P. Wang[6], Wangdui[6], H. R. Wu[4], Q. Wu[6], J. L. Xu[5], L. Xue[9], Z. Yang[4], Y. Q. Yao[5], J. Yin[5], Y. Yokoe[15], Y. L. Yu[4,8], A. F. Yuan[6], L. M. Zhai[5], H. M. Zhang[4], J. L. Zhang[4], X. Zhang[3], X. Y. Zhang[9], Y. Zhang[4], Yi Zhang[30], Ying Zhang[4], S. P. Zhao[4], Zhaxisangzhu[6], X. X. Zhou[10] and Y. H. Zou[4,8]

1 Department of Physics, Hirosaki Univ., Japan.
2 Department of Physics, Shinshu Univ., Japan.
3 School of Astronomy and Space Science, Nanjing Univ., China.
4 Key Laboratory of Particle Astrophysics, Institute of High Energy Physics, CAS, China.
5 National Astronomical Observatories, CAS, China.
6 Department of Mathematics and Physics, Tibet Univ., China.
7 Department of Physics, Hebei Normal Univ., China.
8 Univ. of Chinese Academy of Sciences, China.
9 Institute of Frontier and Interdisciplinary Science and Key Laboratory of Particle Physics and Particle Irradiation (MOE), Shandong Univ., China.
10 Institute of Modern Physics, SouthWest Jiaotong Univ., China.
11 Faculty of Engineering, Yokohama National Univ., Japan.
12 Faculty of Engineering, Kanagawa Univ., Japan.
13 Faculty of Education, Utsunomiya Univ., Japan.
14 Faculty of Systems Engineering, Shibaura Institute of Technology, Japan.
15 Institute for Cosmic Ray Research, Univ. of Tokyo, Japan.
16 Polar Environment Data Science Center, Joint Support-Center for Data Science Research, Research Organization of Information and Systems, Japan.
17 National Center for Space Weather, China Meteorological Administration, China.
18 School of Information Science and Engineering, Shandong Agriculture Univ., China.
19 Department of Astronomy, School of Physical Sciences, Univ. of Science and Technology of China, China.
20 College of Industrial Technology, Nihon Univ., Japan.
21 National Institute of Informatics, Japan.
22 National Institute of Information and Communications Technology, Japan.
23 Department of Mechanical and Electrical Engineering, Shangdong Management Univ., China.
24 College of Science, China Univ. of Petroleum, China.
25 Tokyo Metropolitan College of Industrial Technology, Japan.
26 Department of Physics, Konan Univ., Japan.
27 Shonan Institute of Technology, Japan.
28 Research Institute for Science and Engineering, Waseda Univ., Japan.
29 Japan Atomic Energy Agency, TJapan.
30 Key Laboratory of Dark Matter and Space Astronomy, Purple Mountain Observatory, CAS, China.

Tibet Air Shower Array

@Yangbajing in Tibet, China (90.522° E, 30.102° N, 4,300 m a.s.l.)

This presentation uses data from Nov 1999 to May 2010

Scintillation Counter Array : 0.5 m^2 x 789 counters
Effective area : ~ 37,000 m^2
Energy range : ~ TeV - 100 PeV
F.O.V. : ~ 2 sr

Relative timing information ➡ **Arrival direction**
Angular Resolution ~0.4° @10TeV

Charge information ➡ **Primary cosmic-ray energy**
Energy Resolution ~70% @10TeV

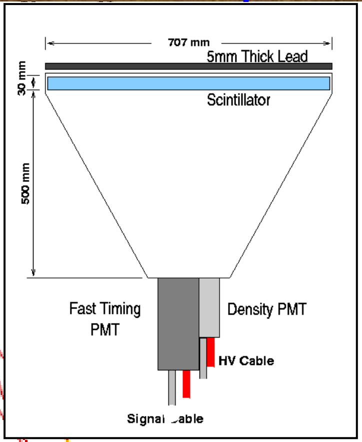

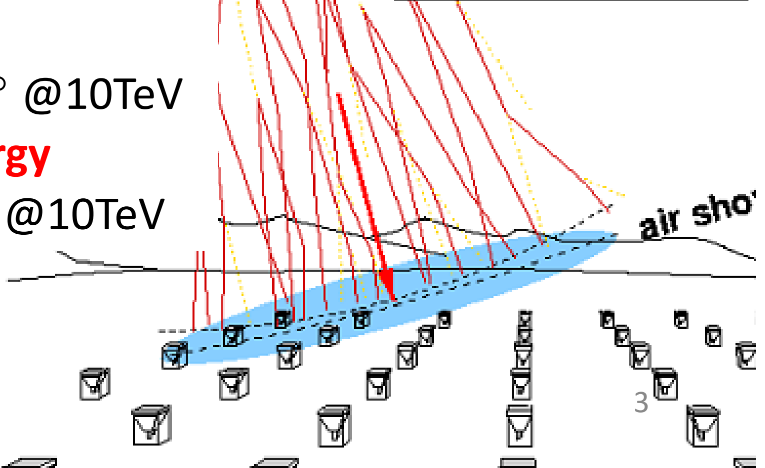

Anisotropy at TeV energies

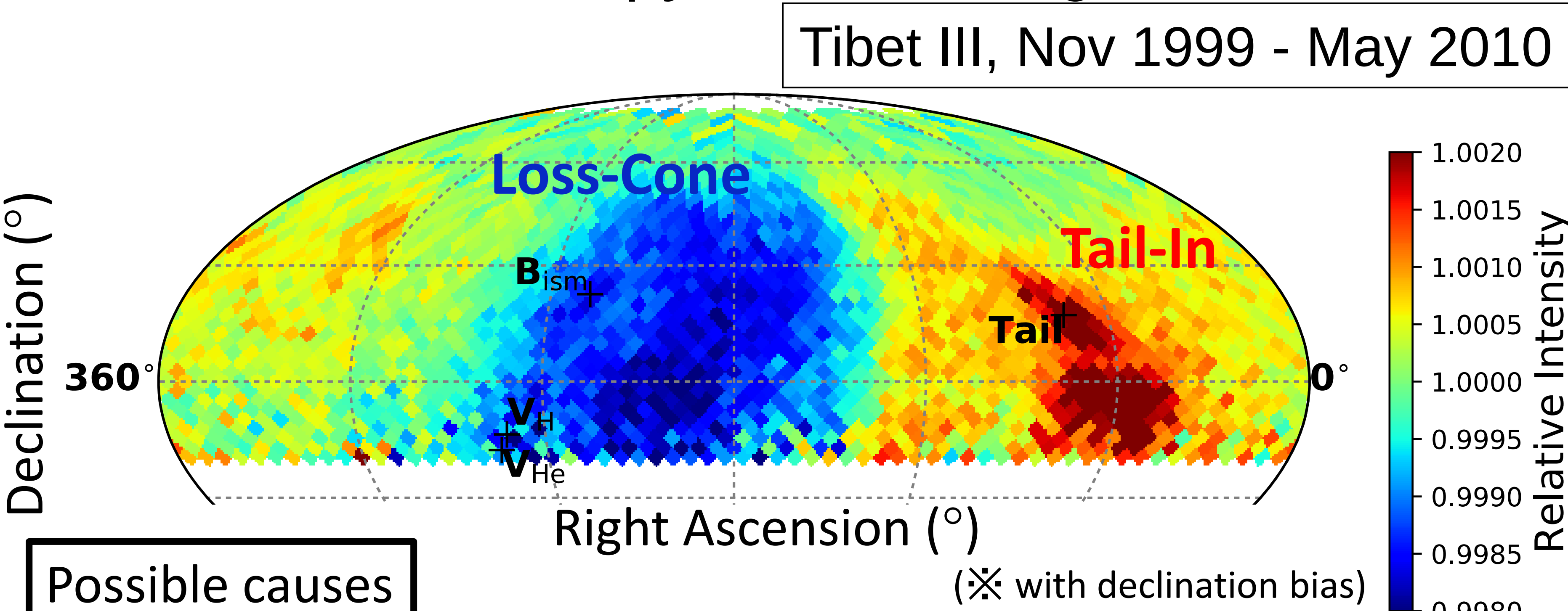

Possible causes

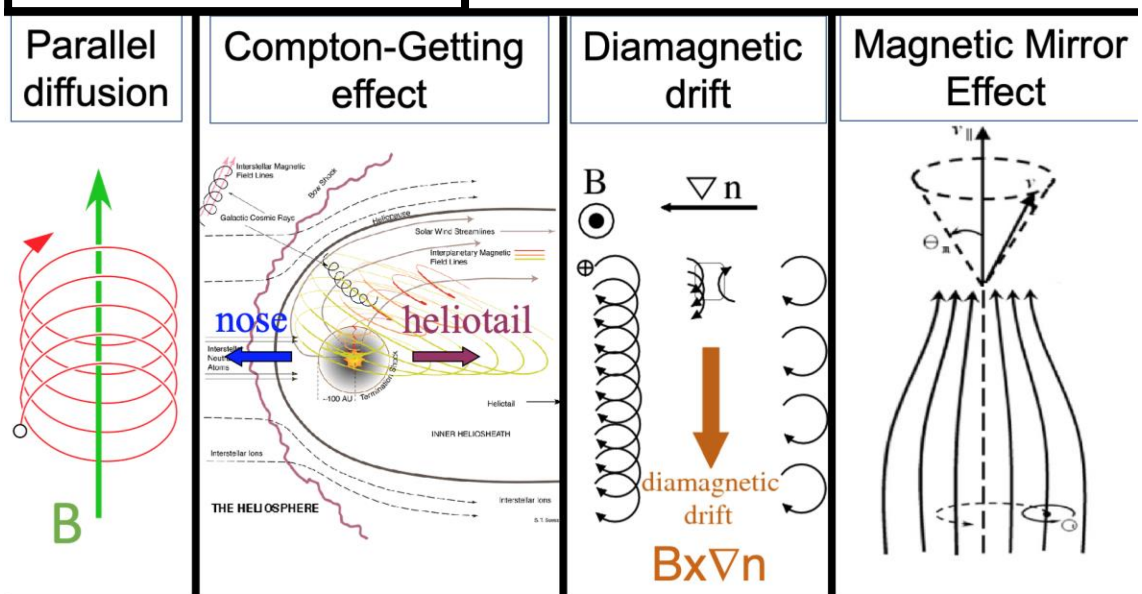

+ heliospheric modulation

Recent study based on intensity mapping (1)

Liouville's theorem

Phase-space density distribution of CRs: $f(\mathbf{r}, \mathbf{p}, t)$

$$Df = \frac{\partial f}{\partial t} + \frac{d\mathbf{r}}{dt} \cdot \frac{\partial f}{\partial \mathbf{r}} + \frac{d\mathbf{p}}{dt} \cdot \frac{\partial f}{\partial \mathbf{p}} = \left(\frac{\partial f}{\partial t}\right)_c \approx 0$$

$$f(\mathbf{r}_E, \mathbf{p}_E, t) \approx f(\mathbf{r}_B, \mathbf{p}_B, t)$$

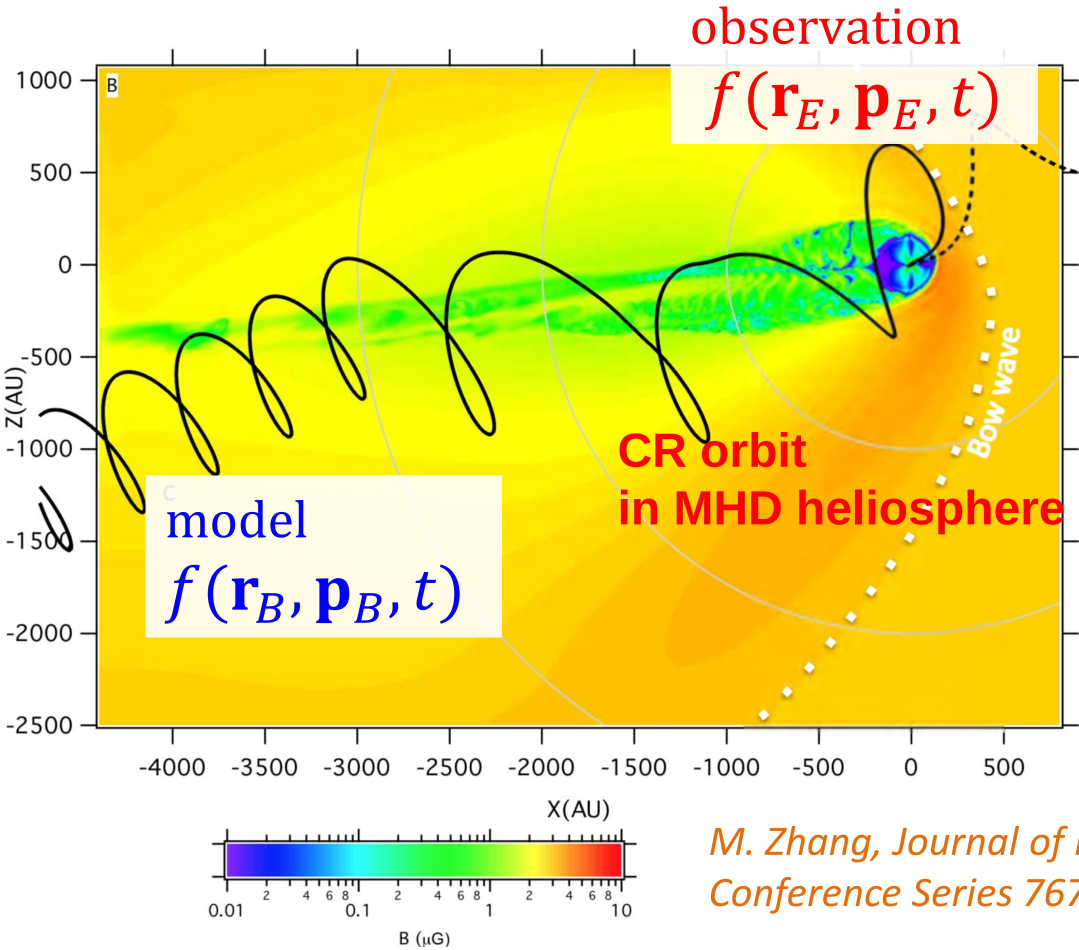

Intensity of CRs with $\boldsymbol{p}_E$ @ Earth

‖

Intensity of CRs with $\boldsymbol{p}_B$ @ Outer Boundary of heliosphere

Mapping of CR intensity between Earth and outer boundary

⇩

CR anisotropy @ outer boundary

M. Zhang, Journal of Physics, Conference Series 767, 012027 (2016)

Recent study based on intensity mapping (2)

Zhang+, ApJ, 889, 97 (2020)

Anisotropy @ Earth

Data

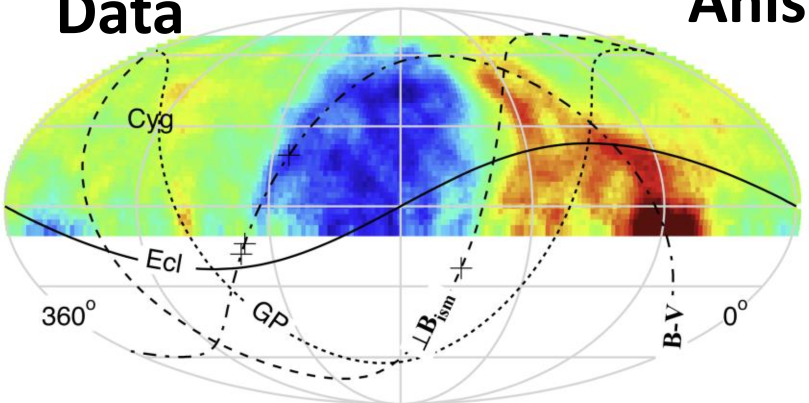

Model

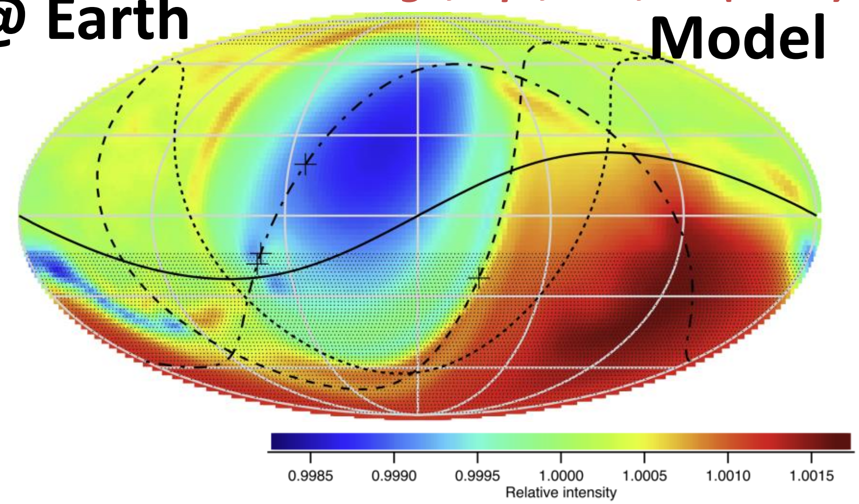

Dipole amplitude along B_{ISM}

Parameter Name	Value
Amplitude of pitch-angle dipole	$A_1 = (0.165 \pm 0.002)\%$
Amplitude of pitch-angle quadrupole	$A_2 = (0.015 \pm 0.002)\%$
CR density gradient	$\lvert G_\perp \rvert = (0.021 \pm 0.001)\%/R_g$
Normalization	$f_0 = 1 + (0.024 \pm 0.001)\%$

(Reduced χ^2 = 4.5)

Dipole amplitude along B_{ISM} x ∇f

Anisotropy @ outer boundary

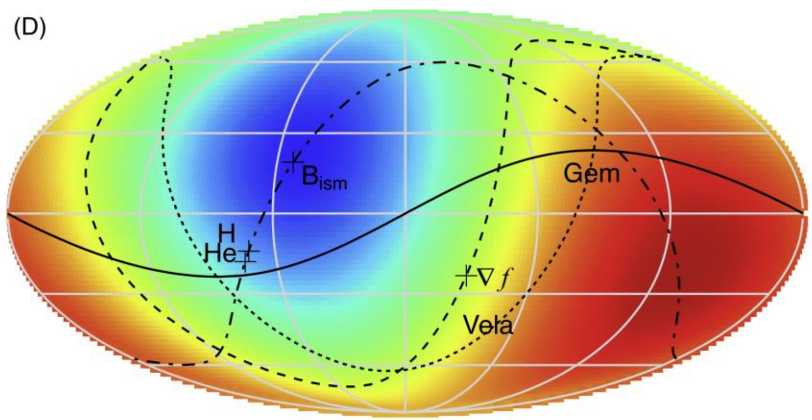

- Dipole amplitude A_1 along B_{ISM} is dominant
- CR density gradient direction (∇f) close to Vela

Recent study based on intensity mapping (2)

Zhang+, ApJ, 889, 97 (2020)

Anisotropy @ Earth

Data

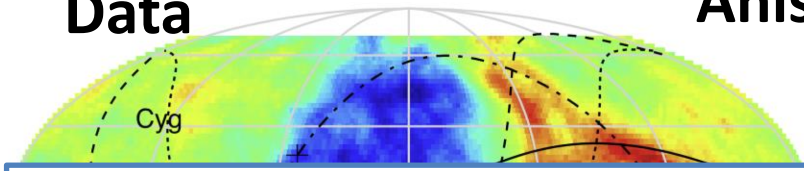

Model

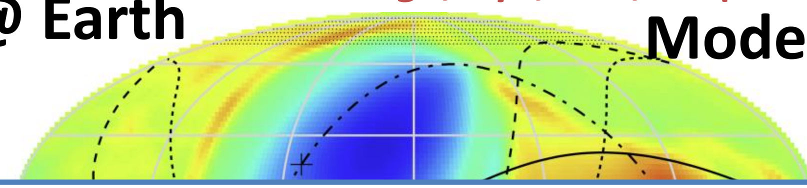

Intensity mapping using only 4 TeV monoenergy protons

⬇

CR energy spectrum & composition must be considered

Parameter Name	Value
Amplitude of pitch-angle dipole	$A_1 = (0.165 \pm 0.002)\%$
Amplitude of pitch-angle quadrupole	$A_2 = (0.015 \pm 0.002)\%$
CR density gradient	$\lvert G_\perp \rvert = (0.021 \pm 0.001)\%/R_g$
Normalization	$f_0 = 1 +$ ...

(Reduce

Dipole amplitude along B_{IS}

Anisotropy @ outer boundary

Reduced χ^2 = 4.5

⬇

Modeling must be improved

MHD model heliosphere used in this work

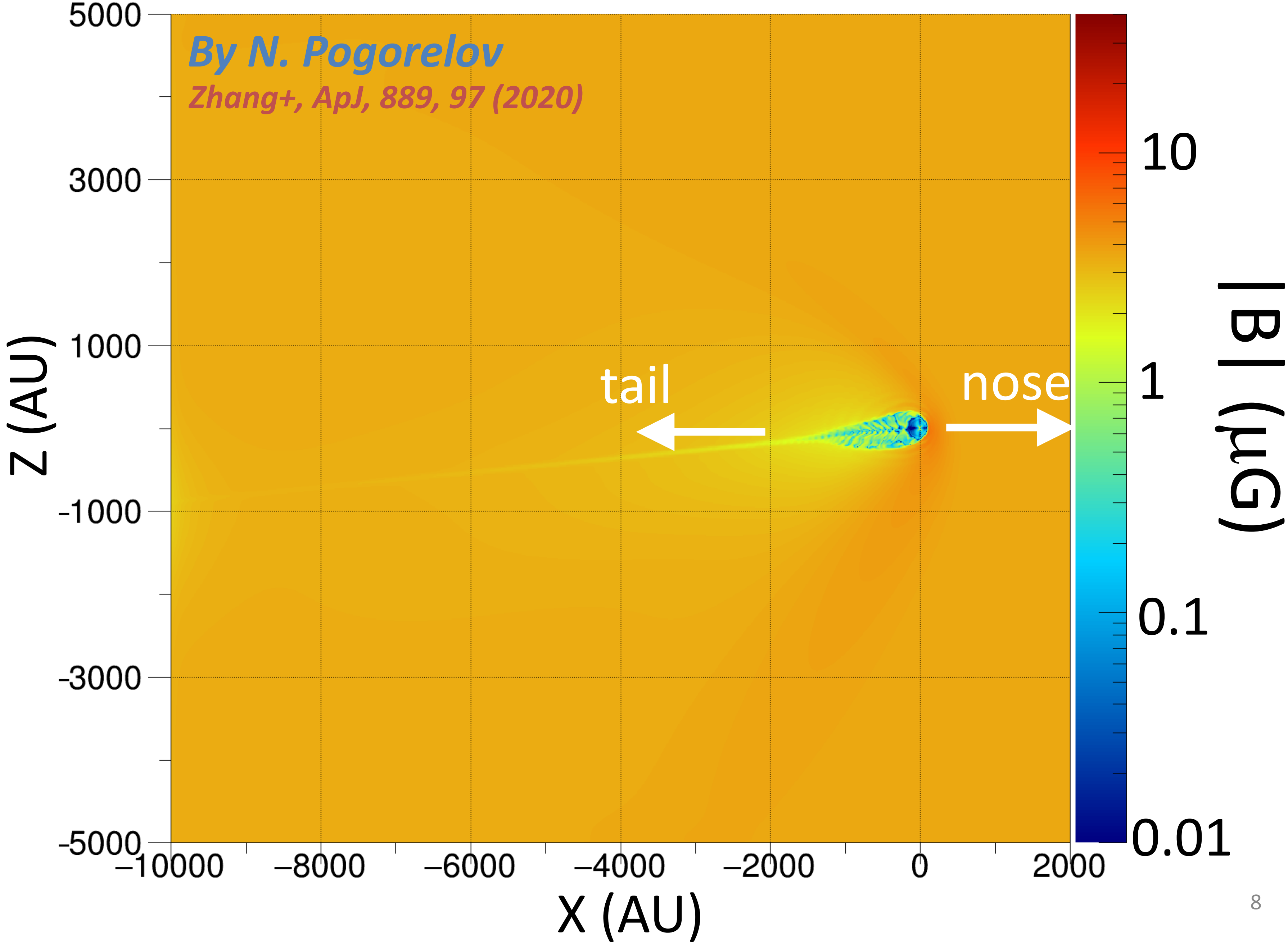

Intensity mapping method

- Set Earth at 4 positions (±1AU, 0, 0), (0, ±1 AU, 0)
- Shoot CR particles with reversed charge into MHD heliosphere
  - — initial directions (4 samplings for each data pixel)
  - — Observed rigidity distribution taken into account
- Record CR momentum directions @ outer boundary
  - — Boundary defined as a surface where:

    Deviation in $\overrightarrow{B}_{\rm helio}$ strength from $\overrightarrow{B}_{\rm ISM}$ < 0.1%, and

    Deviation in $\overrightarrow{B}_{\rm helio}$ direction from $\overrightarrow{B}_{\rm ISM}$ < 0.1°

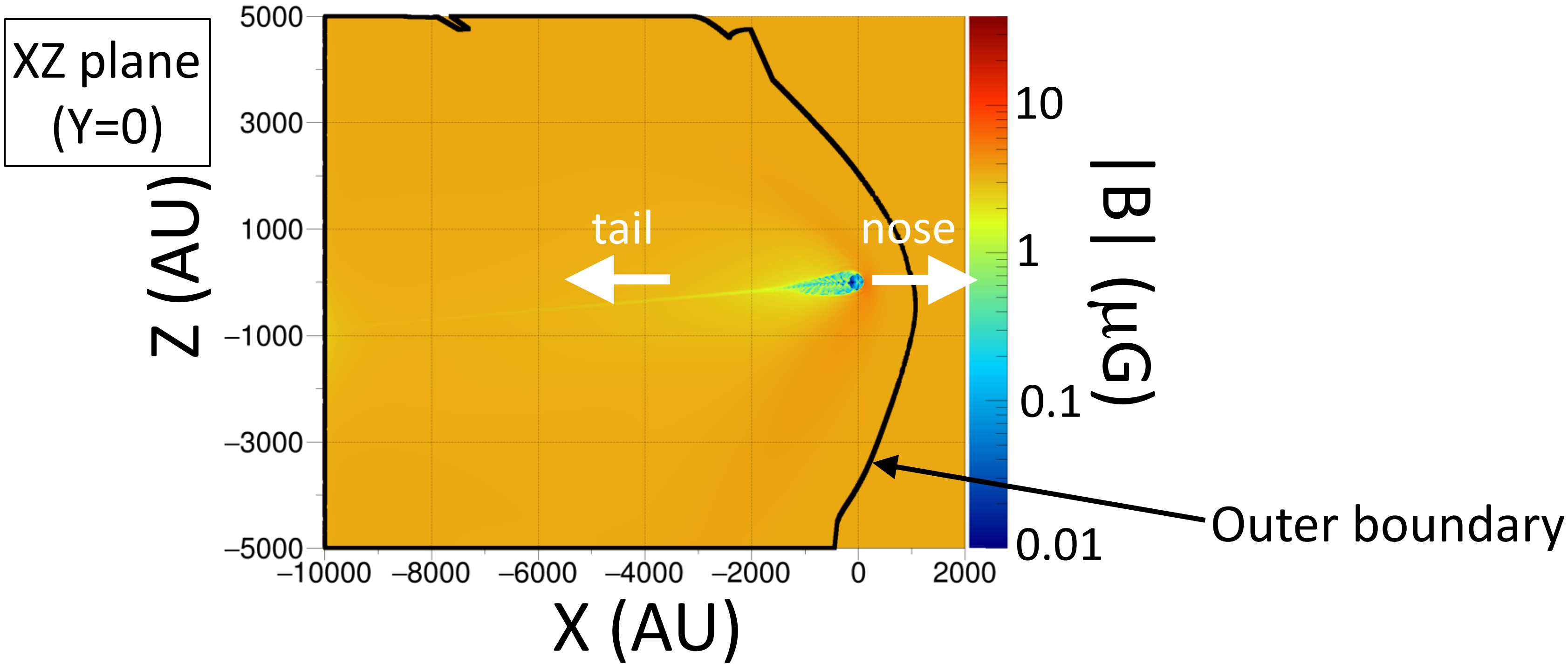

Energy spectrum & composition

Evaluate how different CR species with different energies contribute to the observed anisotropy using MC sim.

- CR energy spectrum & composition based on direct measurements

M.Shibata+, ApJ, 716, 1076 (2010)

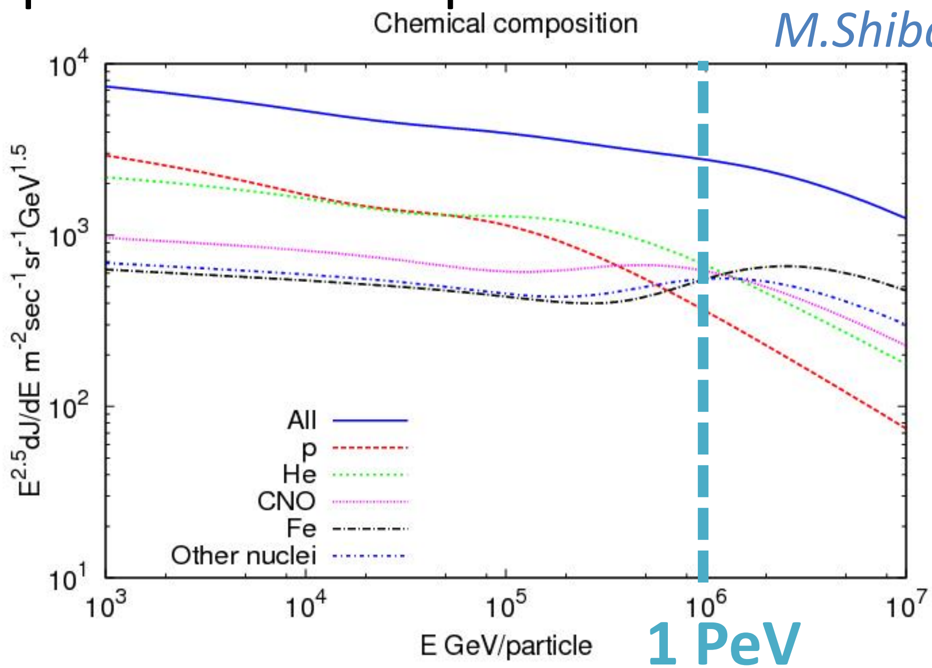

- Air shower generation and Air Shower array response simulation
- Analyze MC events in the same way as experimental data

➡ **Evaluate weight factor**

Weight factor for each declination band (MC)

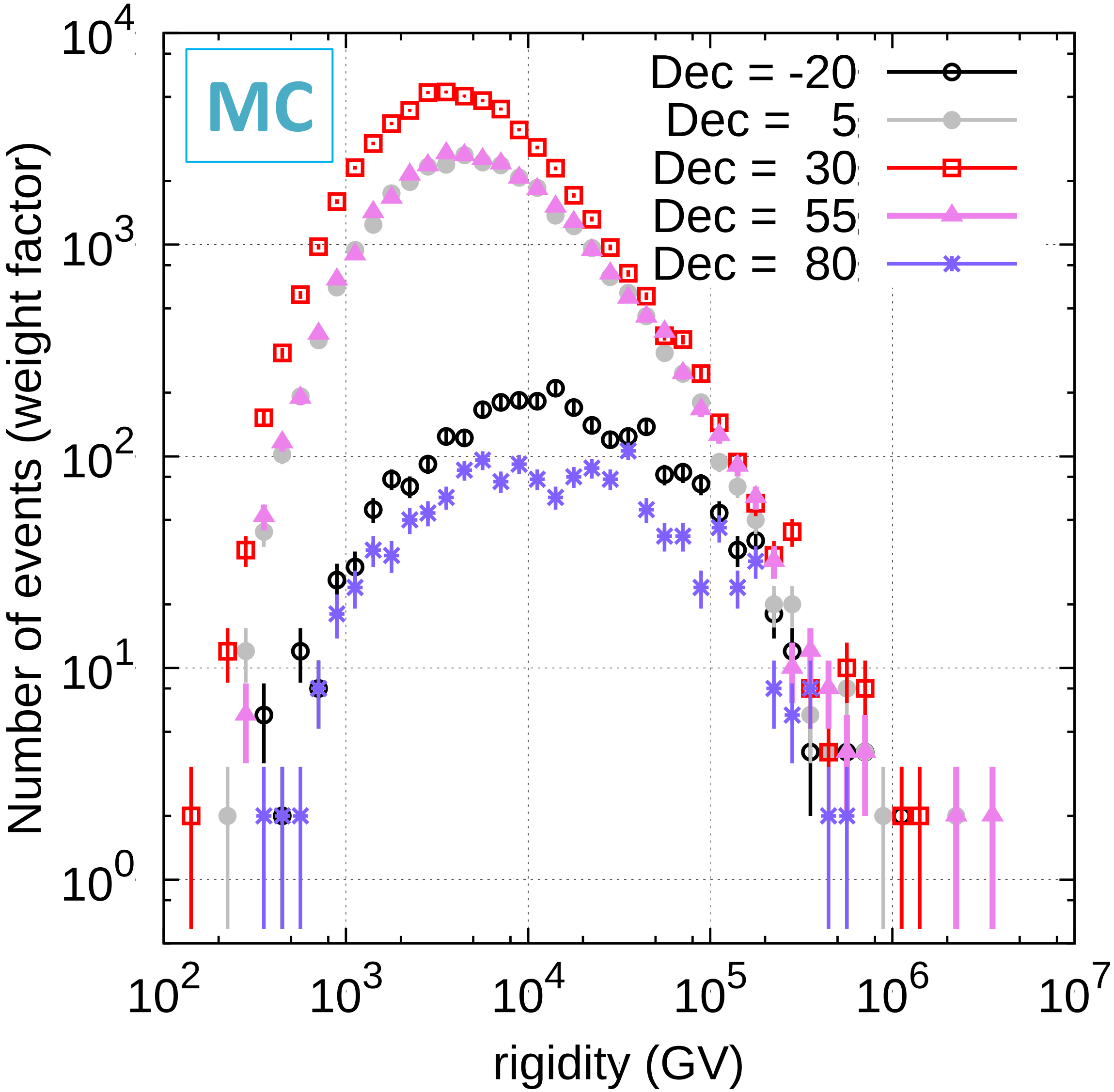

How to derive anisotropy @ outer boundary

1) Assume a model of relative intensity @ outer boundary as:

$$I_{\rm ISM} = 1 + A_{1||}\cos(\mu_2) + A_{2||}\cos^2(\mu_2) + A_{1\perp}\cos(\mu_1) + I_{\rm CG}$$

- μ_2: pitch angle
- μ_1: angle between particle's $\vec{p}$ and $\vec{B}_{\rm ISM} \times \nabla n$
- $A_{1||}$: dipole amplitude parallel to $\vec{B}_{\rm ISM}$
- $A_{2||}$: quadrupole amplitude parallel to $\vec{B}_{\rm ISM}$
- $A_{1\perp}$: dipole amplitude perpendicular to $\vec{B}_{\rm ISM}$
- $I_{\rm CG}$: Compton-Getting anisotropy due to heliospheric motion relative to ISM ($v = 23.2$ km/s ➡ amplitude 0.03%)

∗ $\vec{B}_{\rm ISM}$: (R.A., Dec) = (232.5°, 19.0°)

2) Map $I_{\rm ISM}$ to Earth

3) Normalize the average of mapped model intensity @ Earth to one for each decl. band

4) Calculate χ^2 between normalized model intensity and experimental data

➡ Repeat 1) – 4) and obtain best-fit parameter values that minimize χ^2

4 free parameters: $A_{1||}$, $A_{2||}$, $A_{1\perp}$, α_1

(α_1, δ_1): direction of ∇n (CR density gradient perpendicular to $\vec{B}_{\rm ISM}$)

Results: fitting by dipole & quadrupole flows

$$I_{\rm ISM} = 1 + A_{1\parallel}\cos(\mu_2) + A_{2\parallel}\cos^2(\mu_2) + A_{1\perp}\cos(\mu_1) + I_{\rm CG} \quad (\alpha_1, \delta_1) : \text{direction of } \nabla n$$

Dipole amplitude along B_{ISM} **Dipole amplitude along $B_{ISM} \times \nabla n$** χ^2 / ndf = 3320 / 2052 = **1.62**

$A_{1\parallel}$ (%)	$A_{2\parallel}$ (%)	$A_{1\perp}$ (%)	α_1 (°)	δ_1 (°)
0.234 ± 0.002	0.011 ± 0.004	0.131 ± 0.006	137.5 ± 1.4	14.2 ± 3.8

Data@Earth

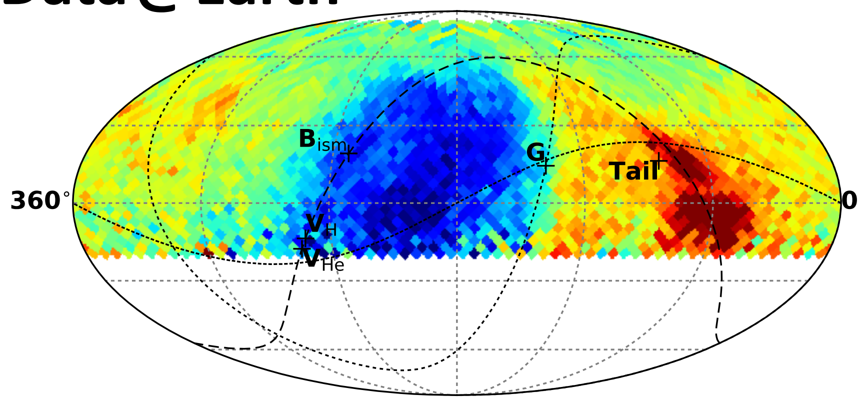

Model@Earth

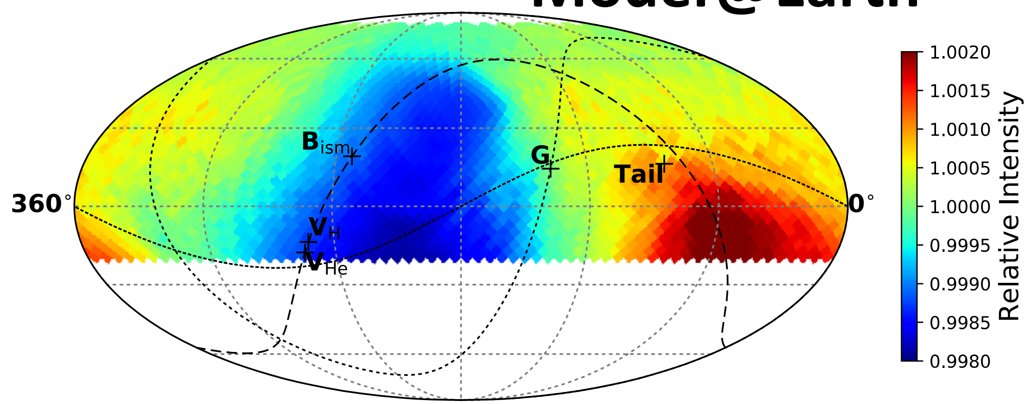

Model @ Boundary

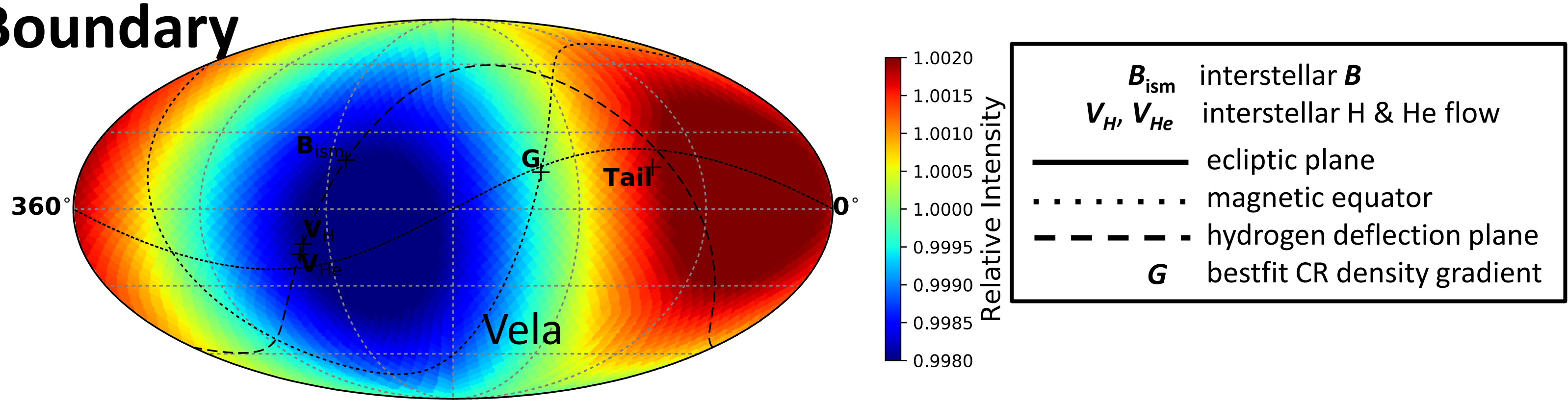

- $A_{1\perp}$ is not so small; about half of $A_{1||}$
- CR density gradient direction (G) not close to Vela

Results: fitting by spherical harmonics

$$I_{\rm ISM}(\theta,\phi) = 1 + \sum_{l=1}^{l_{\max}} \sum_{m=-l}^{l} f_{lm} Y_{lm}(\theta,\phi) + I_{\rm CG}$$

χ^2 / ndf = 1393 / 1432 = **0.973 (76.4 %)**

L_{max} = 24 (624 parameters)

Data @Earth

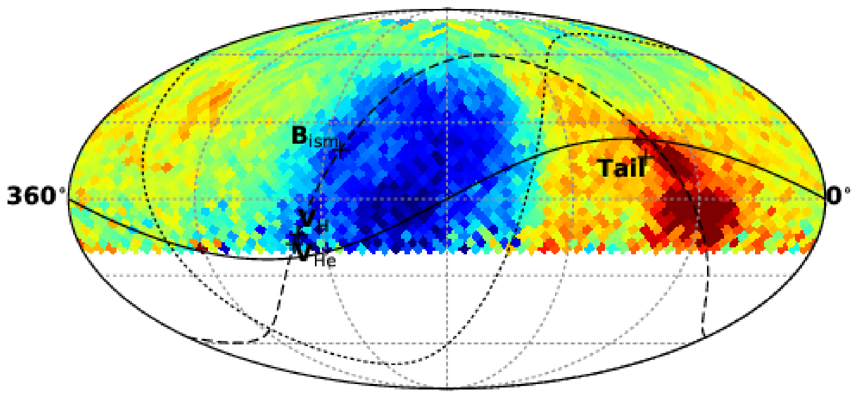

Model Fitting @Earth

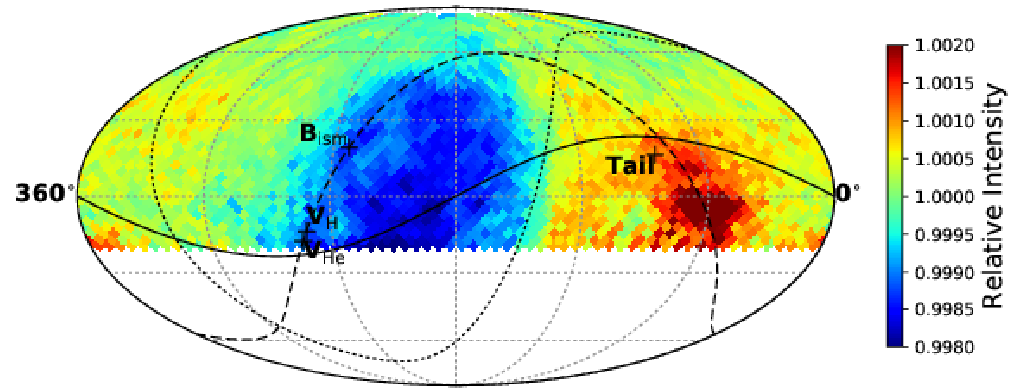

Model @ Boundary

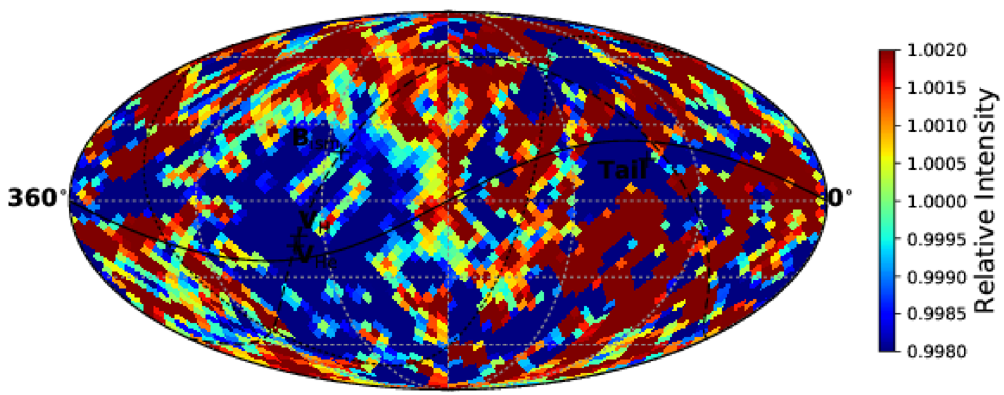

B_{ism} interstellar ***B***
V_H, V_{He} interstellar H & He flow

ecliptic plane
magnetic equator
hydrogen deflection plane

- Unrealistic small-scale anisotropy appears @ outer boundary

Results: Power spectrum

$$C_l = \left(\frac{1}{4\pi}\right)\left(\frac{1}{2l+1}\right)\sum_{m=-l}^{l} f_{lm}^2$$

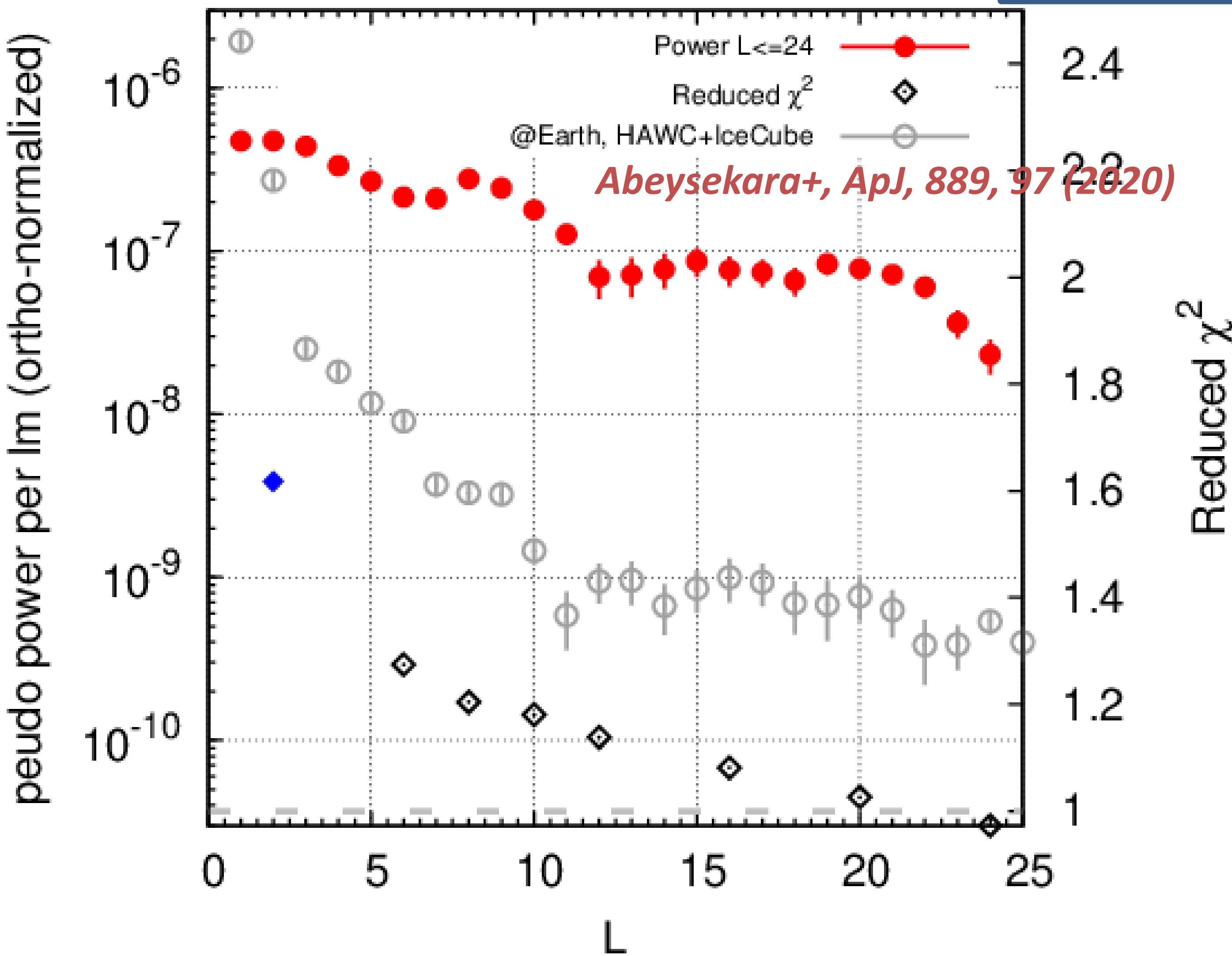

- L ≥ 20 terms are needed @ outer boundary to get reasonable χ^2
- Spectrum flatter @ outer boundary than @ Earth

CR intensity distributions at different boundaries?

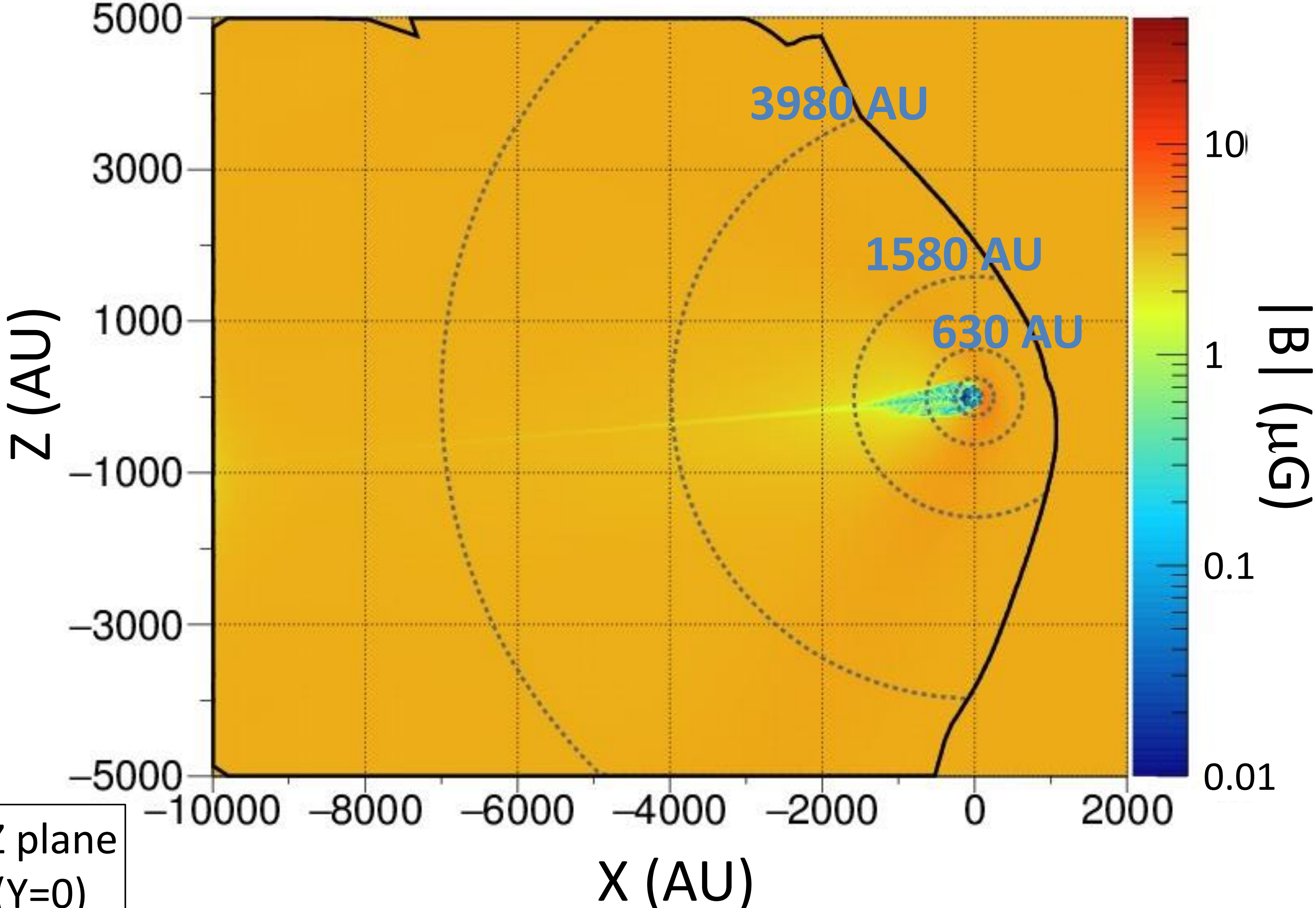

XZ plane
(Y=0)

Results: intensity distributions @ different outer boundaries

Observed at Earth

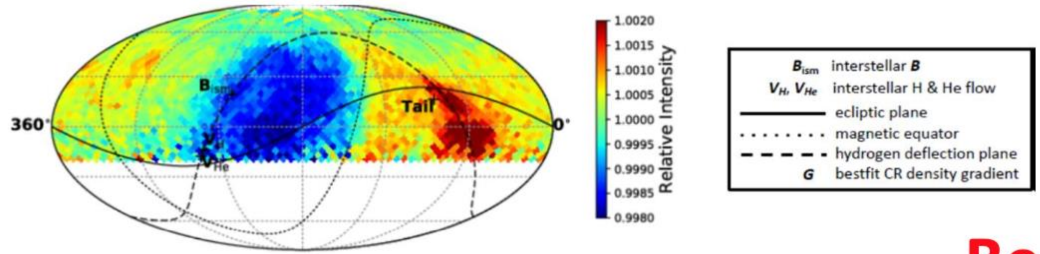

Reproduced at Earth

Best-fit at boundary ($r=r_B$)

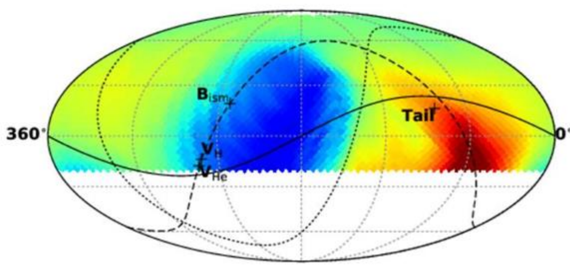

r_B= 630 AU

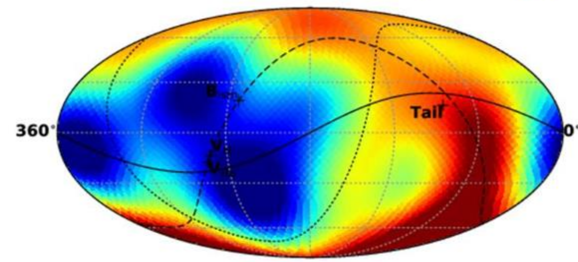

L_{max} = 4 ($N_{param.}$=26)

χ^2 / ndf = 0.962

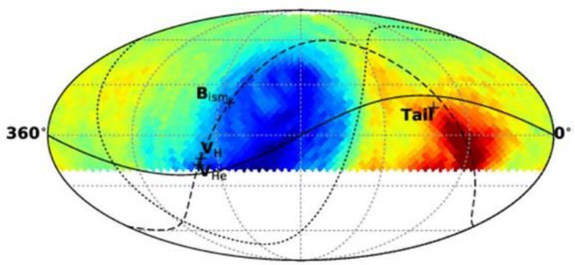

1580 AU

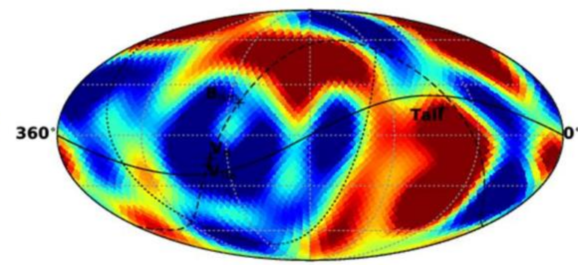

L_{max} = 8 ($N_{param.}$=80)

χ^2 / ndf = 0.982

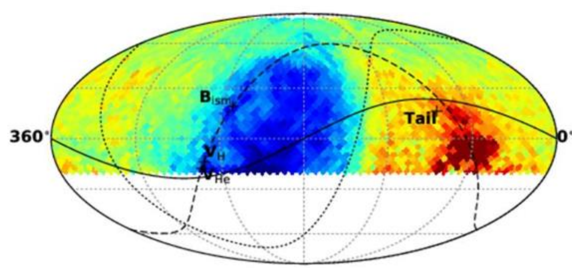

3980 AU

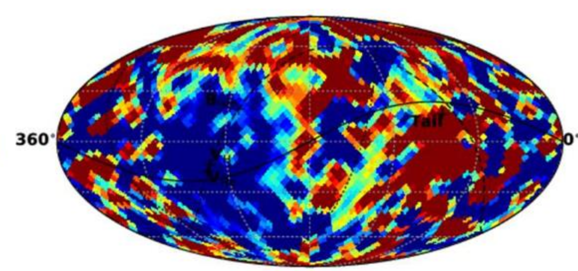

L_{max} = 20 ($N_{param.}$=440)

χ^2 / ndf = 0.942

Effect of particle scattering with magnetic irregularities in the heliosphere ??

Diffusion coefficient

Moskalenko+, ApJ, 565, 280 (2002)

$$D = \beta D_0 \left(\frac{\rho}{\rho_0}\right)^{\delta}$$

$(\beta \approx 1)$

$D_0 = 6.1 \times 10^{28}\ [\mathrm{cm^2 s^{-1}}]$

$\rho_0 = 4\ [\mathrm{GV}]$

$\delta = \frac{1}{3}$

Mean free path

$$D = \frac{1}{3} v L \quad (v \approx c)$$

$L \sim 5 * 10^6$ AU for 7 TeV proton

Assuming $T \sim 60$ days from boundary to Earth

➡ $dl = 1 * 10^4$ AU for 7 TeV proton

➡ $\sqrt{\langle \Theta^2 \rangle} \sim 4^\circ$

Yasue+, Planet Space Sci. 33, 1057 (1985)

The projected angle Θ is defined as the angle between **V** and the projection of the scattered velocity on one of the planes, and has the following probability distribution:

$$\Phi(\Theta) = \frac{1}{\sqrt{2\pi\langle\Theta^2\rangle}} \exp\left(-\frac{\Theta^2}{2\langle\Theta^2\rangle}\right), \qquad (1)$$

where $\langle\Theta^2\rangle$ is the mean square angle of Θ for dl and is related with the scattering mean free path L as

$$\langle\Theta^2\rangle = \left(\frac{\pi}{2}\right)^2 \left(\frac{dl}{L}\right), \qquad (2)$$

in which

$$L(r, P) = L_0 \left(\frac{P}{10\ \mathrm{GV}}\right)^2 \exp\left(\frac{r-1}{33\ \mathrm{a.u.}}\right) (\mathrm{a.u.})$$

$$\text{for } P > 10\ \mathrm{GV}. \qquad (3)$$

The radial dependence of L is quoted from Fulks (1975) and its rigidity dependence is based on a theoretical consideration (Parker, 1958; Jokipii, 1971) and seems to be supported by observations in the low rigidity region ($P \sim 10$ GV) (Fulks, 1975; Lockwood and Webber, 1979; Zusmanovich, 1981). The magnitude of L_0 is set to 0.77 a.u. by the normalization at 10 GV to the one obtained in the lower rigidity region by Garcia-Munoz *et al.* (1977).

Results: best-fit relative intensity distributions

L_{max} = 5 (35 parameters) χ^2/ndf = 2042/2021 = **1.01 (36 %)**

Data @Earth

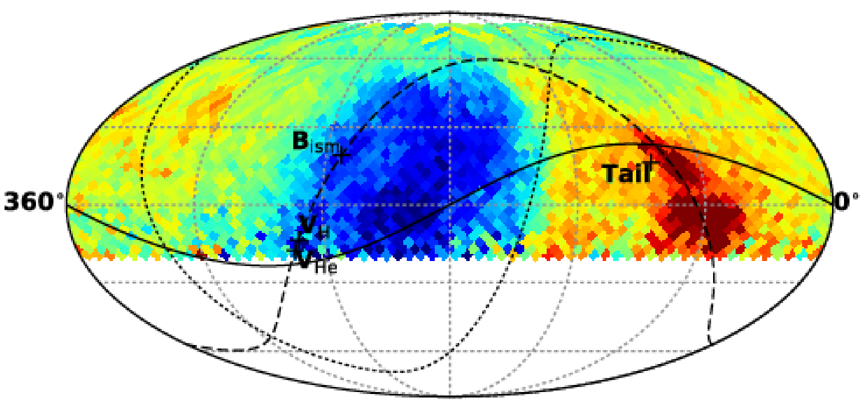

Model Fitting @Earth

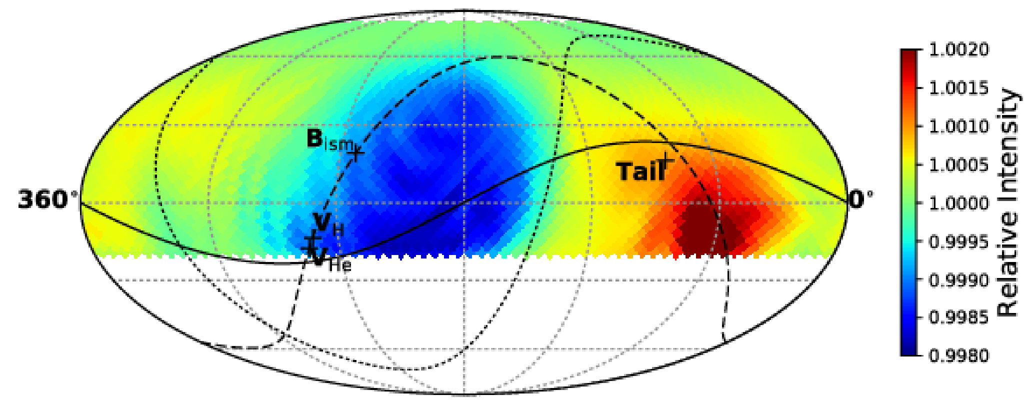

$\boldsymbol{B}_{ism}$	interstellar ***B***
V_H, V_{He}	interstellar H & He flow
———	ecliptic plane
· · · · · · · ·	magnetic equator
— — — —	hydrogen deflection plane
G	bestfit CR density gradient

Model @ Outer boundary

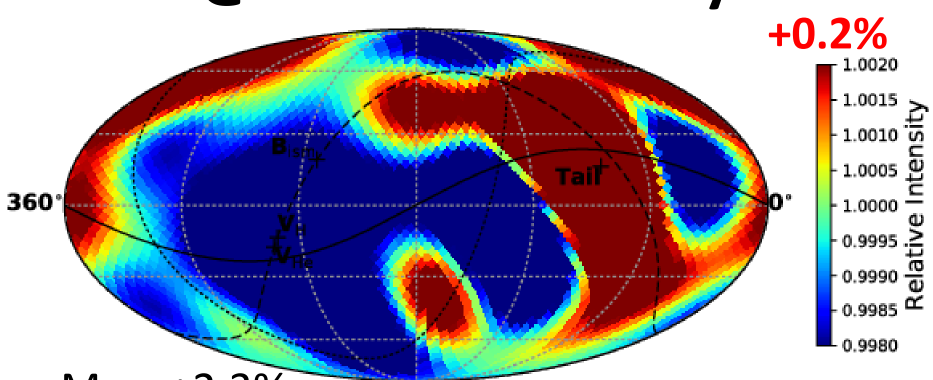

Max: +2.3%
Min: –1.2%

- L ≤ 5 terms are sufficient @ outer boundary to get reasonable χ^2
- Amplitude @ outer boundary becomes percent-level

Results: Power spectrum

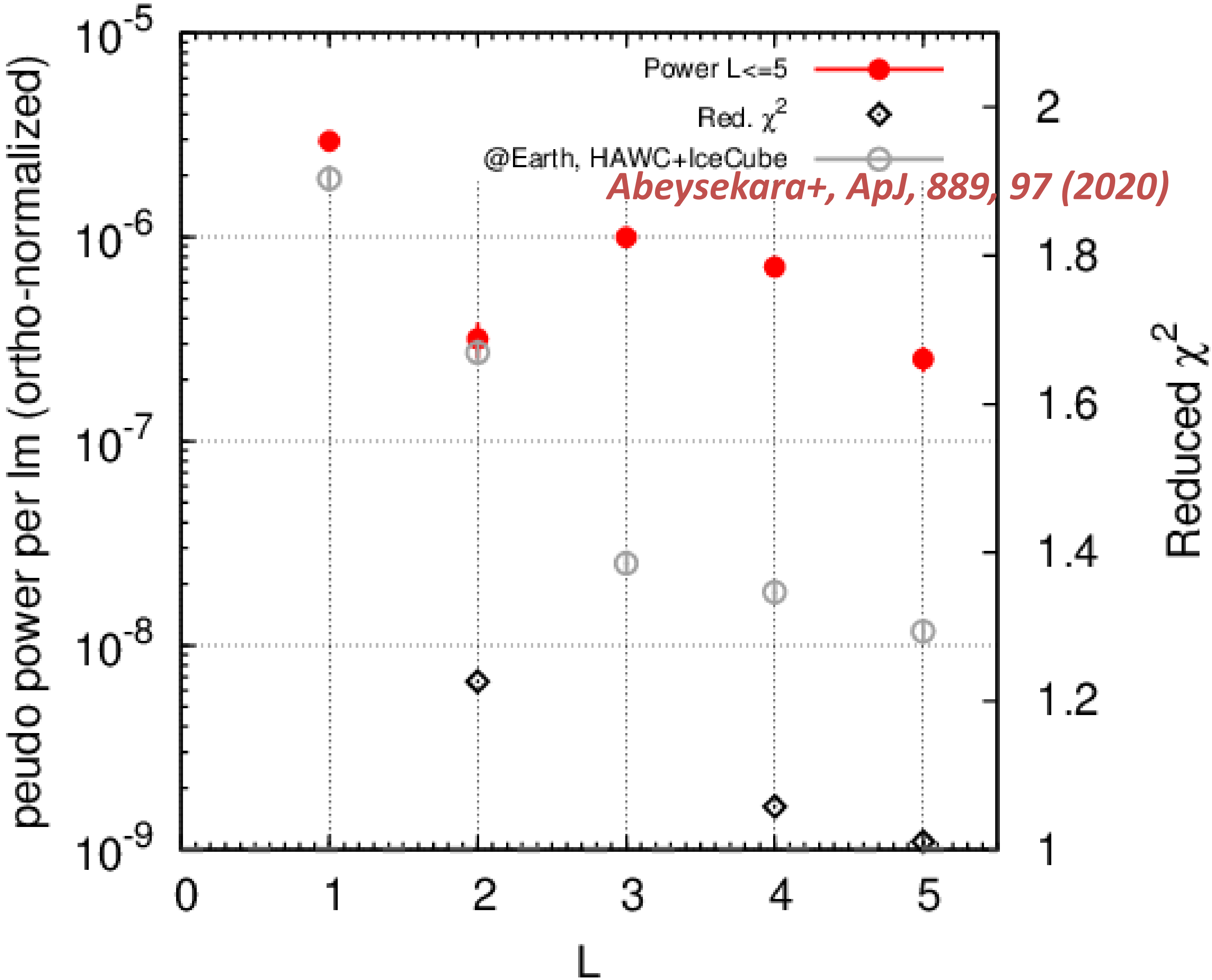

Terms with L ≥ 3 larger @ outer boundary than @ Earth

➡ intensity-mapping method needs more improvement ??

Summary

Quantitative study on the origin of TeV CR anisotropy based on intensity mapping

- ✓ Rigidity distribution of observed CR particles taken into account
- ✓ Modeling @ boundary improved using spherical harmonics
  ➡ Intensity distribution @ boundary needs L ≥ 20 terms to get reasonable χ^2
- ✓ Tentative study of scattering by magnetic irregularities in the heliosphere
  ➡ Intensity distribution @ boundary can be expressed with L ≤ 5 terms
  But still terms with L ≥ 3 larger @ boundary than @ Earth

Future prospects

- ➢ Suppress the apparent high-order terms in the power spectrum
  ➡ Using a "snapshot" MHD model of the heliosphere may be a problem
  (Data covers 10 years (2000-2009) of A<0 phase of 23rd solar cycle)
- ➢ Compare the results with other MHD heliosphere models
  (e.g. by Washimi+ and Opher+)
- ➢ Examine the observed energy dependence of anisotropy around 100 TeV

Thank you
for you attention!

Distribution of the time from Earth to Boundary

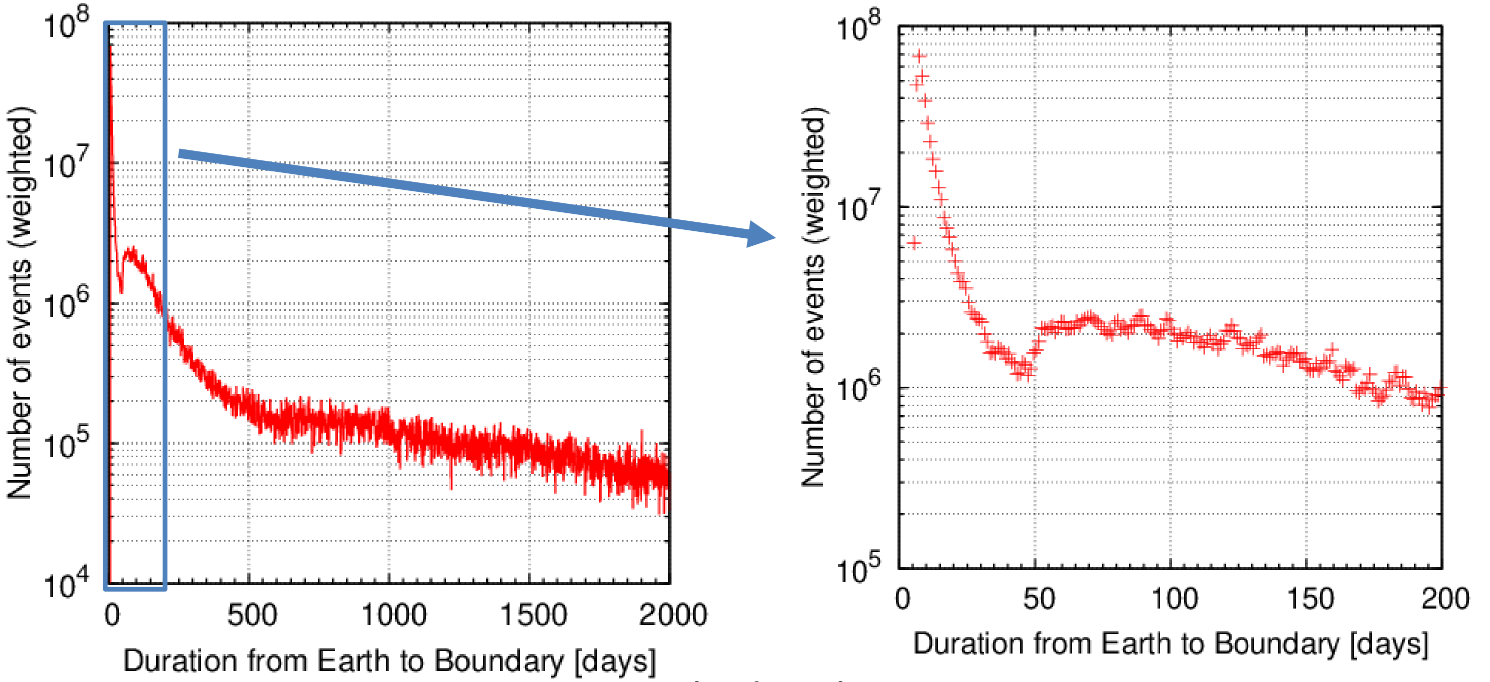

Scattering angle distribution

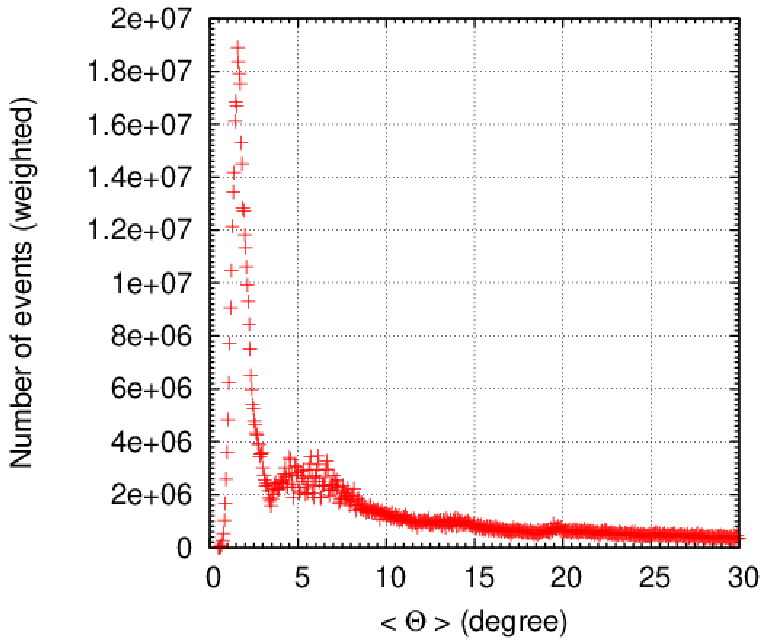

Washimi MHD model A

A < 0

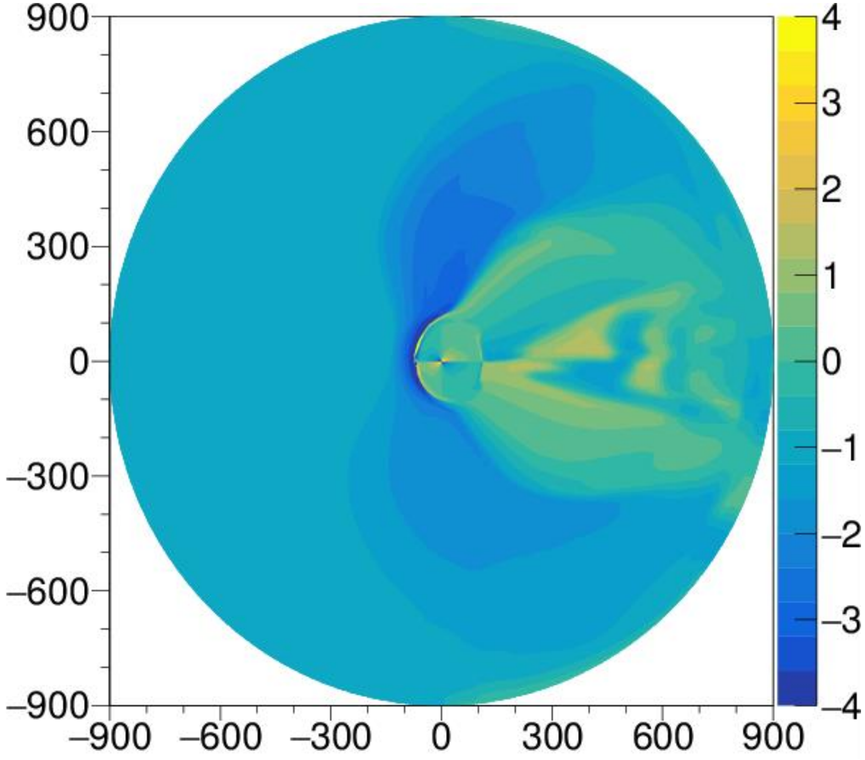

Washimi MHD model B

A > 0

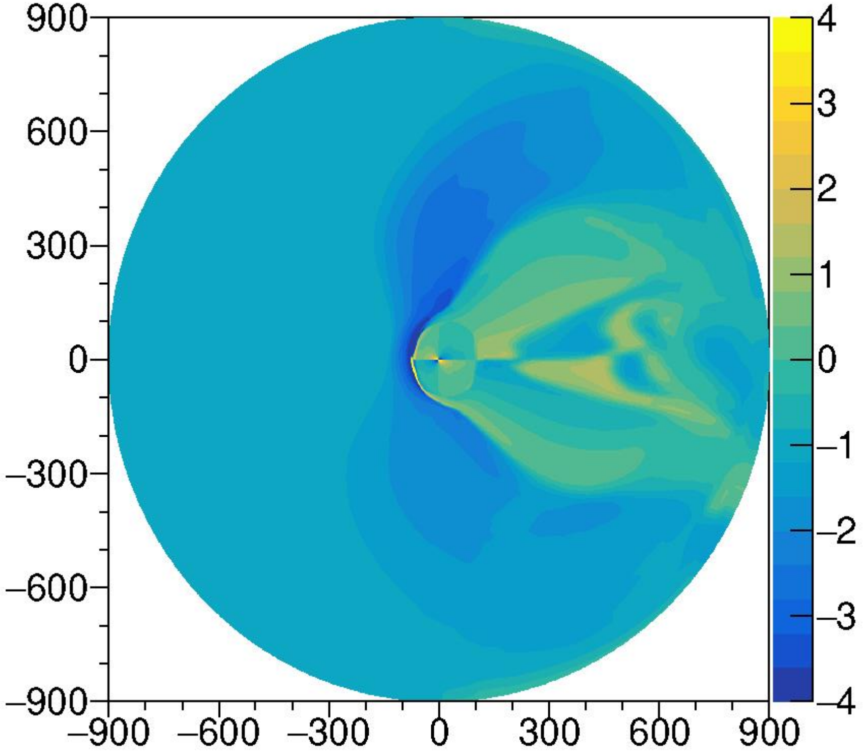

Power spectrum

$$C_l = \left(\frac{1}{4\pi}\right)\left(\frac{1}{2l+1}\right)\sum_{m=-l}^{l} f_{lm}^2$$